RSC Advances

ROYAL SOCIETY
OF **CHEMISTRY**

www.rsc.org/advances

Facile synthesis of BiOI/CdWO$_4$ p-n junction: Enhanced

Photocatalytic Activities and Photoelectochemistry

Yi Feng, Chunbo Liu, Jibin Chen, Huinan Che, Lisong Xiao, Wei Gu, Weidong Shi*

School of Chemistry and Chemical Engineering, Jiangsu University, Zhenjiang, 212013, P. R. China.

Corresponding author: Tel: +86 511 8879 0187   Fax. : +86 511 8879 1108

E-mail address: swd1978@ujs.edu.cn

Abstract

In this work a series of novel BiOI/CdWO$_4$ p-n junction photocatalysts were successfully fabricated via a facile step of ultrasonic and stirring process. The photodegradation tests exhibit that the BiOI/CdWO$_4$ p-n junction photocatalytic show efficiency enhanced than pure BiOI and CdWO$_4$. The best photocatalytic performance was obtained for the sample of BC-2.0, and the as prepared samples were studied by XRD, TEM, HRTEM, XPS, UV-vis DRS and photoluminescence (PL) spectroscopy. The enhancement predominantly could be attributed to the improving photogenerated electron-hole separation and migration efficiency of the synergy impact between BiOI and CdWO$_4$. The efficient separation of electron-hole pairs because of the synergy impact between BiOI and CdWO$_4$. Radical scavenger experiments and ESR investigated indicate that holes (h$^+$) and superoxide radicals ($\cdot$O$_2^-$) were the main active species in the photocatalytic process.

Keywords: ultrasonic and stirring reaction; p-n junction; BiOI/CdWO$_4$; visible-light; photocatalytic

1. Introduction

Water pollution is a challenging environmental issue in the modern industrial society has been attracting massive research interest [1-5]. At present, it is a serious challenge by human beings to removal of organic pollutions from wastewater. To solve environmental pollution lots of research been explored. However, these technologies still have some problems for application in practice, such as secondary pollution or unsatisfactory treatment. Thankfully, semiconductor catalysts been successfully applied in photocatalysis bringing the gospel to the people effective solving our current environmental pollution problems [6-8]. $CdWO_4$ is one of the most promising catalysts has been widely investigated in photocatalysis for the optical, chemical and structural properties [9, 10]. However, the individual of $CdWO_4$ with wide band gap response to only under UV light with (<5%) and the charge recombination strongly hinders its application upon visible light irradiation. In order to prolong light absorption into the visible light range, much strategies have been attempt, such as noble metal loading and coupling with other semiconductors form a heterojunction, have been proposed to enhance the photoactivity of $CdWO_4$. Hence, a strategy of focusing on coupling $CdWO_4$ with other narrow bandgap semiconductors to form efficient and visible light-responsive composite photocatalysts at the interface have been investigated widely. Imran synthesized $WO_3/CdWO_4$ and the photodegradation efficiency of Methyl Blue (MB) was enhanced [11]. Xu team prepared $CdS/CdWO_4$ and concluded that the formed heterojunction could separate the photogenerated carriers efficiently [12]. Hence, increasing efforts are focused on researching narrow bandgap

semiconductors coupling with $CdWO_4$ to form efficient and visible light-responsive heterojunction composite photocatalysts.

Recently years, bismuth oxyhalides (BiOX, X=Cl, Br, and I) have been arisen much attention due to their potential used in photocatalysts [13-15]. Among of them, BiOI is a typical narrow bandgap semiconductor photocatalyst serving as member of the Aurivillius family composed of alternate $Bi_2O_2^{2+}$ and I^- layer with a narrow band gap approximate of 1.91 eV, have received more attention for this good visible light absorption ability [16-18]. However, it is a pity that high recombination rates of photogenerated charge carriers showed poor lead to the single BiOI with low photocatalytic activity [19-20]. Therefore, enhancing photocatalytic activity of BiOI needs further study. As a typical p-type semiconductor, BiOI can serve as an efficient visible-light photosensitizer for n-type TiO_2 with a large band gap to greatly enhance its photocatalytic efficiency [21]. $CdWO_4$ is also an n-type semiconductor with a band-gap energy (about 3.2 eV) similar to that of TiO_2. Some studies have reported that $CdWO_4$ exhibited better efficiency than TiO_2 in the photocatalytic degradation of organic pollutants and photoelectric conversion [22-23]. However, although much work has been done, it is still a challenge to develop an inexpensive facile method for the fabrication BiOI-base heterojunction photocatalysts with high visible-light photocatalytic ability. However, to the best of our knowledge, there is no report on the design and fabrication of coupled $BiOI/CdWO_4$ heterostructures and their photocatalytic performances. Based on the prefer literature reports about the synthesis

method of ultrasonic agitation [24-27], we firstly propose the preparation and characterization of BiOI/CdWO$_4$ composite photocatalysts.

Herein, a series of BiOI/CdWO$_4$ composites were prepared by low-temperature and been successfully used as photocatalysts for the photocatalytic degradation of organic pollutants tetracycline(TC) and RhB(Rhodamine B) under visible-light ($\lambda \geqslant$ 420 nm) irradiation. The results exhibited that the BiOI/CdWO$_4$ heterojunction efficiently improving the photocatalytic activity compared with single BiOI and CdWO$_4$, respectively. The activity enhancement was mainly ascribed to the p-n heterojunction, which could facilitate the interfacial charge transfer and improve photogenerated electron-hole pair separation. Moreover, the possible mechanism for the enhanced photocatalytic activity was also proposed on the basis of the obtained experimental results.

2. Experimental

2.1. Materials

Bismuth nitrate hydrate (Bi(NO$_3$)$_3$·5H$_2$O), potassium iodide (KI), Sodium tungsten oxide (Na$_2$WO$_4$ • 2H$_2$O), Nitric acid (HNO$_3$) were purchased from Shanghai Chemical Plant or Tianjin Chemical Plant. All the reagents were analytically grade and used without further purification. Deionized water was used in all experiments.

2.2. Preparation of CdWO$_4$

In a typical synthesis procedure, a certain amount of Na$_2$WO$_4$ • 2H$_2$O (2mmol) was dissolved homogeneously in 20mL of deionized water to form a transparent solution with stirring 10 min marked as A. Then, a certain quality of chromium

acetate was added in 15ml of deionized water marked as B. The next was B solution

added into A solution drop by drop then transferred to a 40 mL Teflon-lined autoclave.

Subsequently, the autoclave was heated to 160 ^{o}C in an oven. After crystallizing for

24 h, the resulting products were filtered, washed with ethyl alcohol and distilled

water for several times, and dried at 60 ^{o}C for the next use.

2.3. Preparation of BiOI/CdWO$_4$ p-n junction

Weighing a certain amount of CdWO$_4$ (0.2g) dissolved in 50ml deionized water

with stirring 30 min. And then a certain amount of KI (1.0 mmol, 2.0 mmol, 3.0 mmol)

was added in the composition. After 30 min stirring, different amount of

Bi(NO$_3$)$_3$·5H$_2$O (keeping 1:1 in molar r atios with KI) were added above the mixed

solution. Ultrasonic and stirring at room temperature for 2h, the resulting products

were filtered, washed with ethanol and distilled water several times, and dried at 60

^{o}C (named as BC-1.0, BC-2.0, BC-3.0 respectively). For comparison, the BiOI/TiO$_2$

(BT-2.0) p-n junction powder was also prepared via the same process of BC-2.0.

2.4 Characterization of photocatalysts

All of the phase compositions and crystal structures of the prepared samples

were determined by powder X-ray diffraction (XRD) method using Cu Kα radiation

(λ = 1.54178 Å), (D/MAX-2500 diffractometer, Rigaku, Japan) with Cu-Kα radiation

source (k = 1.54056) over the 2θ range of 5.0-80º at a scanning rate of 7.0º min^{-1}.

The morphology of prepared samples was observed by scanning electronic

microscopy (SEM) on an S-4800 field emission SEM (SEM, Hitachi, Japan). The

transmission electron microscopy (TEM) and high resolution electron microscopy

(HRTEM) images were taken with a JEOL JEM-2010 electron microscope. Were also used to characterization the samples by transmission electron microscopy (TEM: JEM-2010, Japan). The X-ray photoelectron spectroscopy (XPS) was obtained by a Thermo ESCALAB 250X (America) electron spectrometer using 150 W Al Kα X-ray source. The UV-vis diffused reflectance spectra (DRS) of the samples were obtained from an UV-vis spectrophotometer (UV-2450, Shimadzu, Japan), $BaSO_4$ was used as a reflectance standard. The photoluminescence (PL) spectra of samples were measured on a Perkin-Elmer LS 55 at room temperature using a fluorescence spectrophotometer.

2.5 Photocatalytic activity

The photocatalytic properties of the as-prepared samples were evaluated using TC and RhB organic pollution as a model compound. In experiments, the TC and RhB solution (0.1 g/L, 100 mL) containing 100 mg of photocatalyst were mixed in a quartz reactor. A 300 W Xe lamp ($\lambda > 420$ nm) was employed to provide visible light irradiation. A 420 nm cut-off filter was inserted between the lamp and the sample to filter out UV light ($\lambda < 420$ nm). Prior to visible light illumination, the suspension was strongly magnetically stirred for 30 min in the dark for adsorption/desorption equilibrium. Then the solution was exposed to visible light irradiation with magnetic stirring. At given time intervals, about 5 mL of the suspension was periodically withdrawn and analyzed after centrifugation. The TC and RhB concentration was analyzed by a UV-2550 spectrometer to record intensity of the maximum band at 553

nm in the UV-vis absorption spectra. The degradation efficiency (%) was calculated as follows:

Degradation (%) = $(C_0-C)/C_0\times100\%$ (1)

Where C_0 is the initial concentration of TC and RhB, and C is the time-dependent concentration of dye upon irradiation.

2.6 Active species trapping

Experiments for detecting the active species during photocatalytic reactivity, some sacrificial agents, such as isopropanol (IPA), disodium ethylenediamine tetraacetic acid (EDTA-2Na) and 1, 4-benzoquinone (BQ) were used as the hydroxyl radical (•OH) scavenger, hole (h^+) scavenger and superoxide radical (•O_2^-) scavenger, respectively. The method was similar to the former photocatalytic activity test with the addition of 1mmol of quencher in the presence of RhB.

3. Results and discussion

XRD analysis was used to determine the crystalline phases of the as-prepared catalysts. The composition of BiOI, $CdWO_4$ and $BiOI/CdWO_4$ heterojunction composition were displayed in Figure1. From Figure1, we can obtain that the diffraction peaks are well indexed to the phase $CdWO_4$ structure (JCPDS file No. 39-0256) and BiOI phase (JCPDS card 06-0505), respectively. At the same time no apparent other peaks are be observed, indicating that highly crystalline nature of all the samples. For the $BiOI/CdWO_4$, the diffraction peaks of the composition increase gradually along with the increased BiOI contents in $BiOI/CdWO_4$, while the peaks of

CdWO$_4$ fade away, which may be BiOI added in the solution. The result can also be found in similar systems [28].

The micrographs of the samples were analysis by SEM, and EDS, and the results as shown in Figure2. The Figure 2a and 2b show the different enlarged scale of CdWO$_4$ made up of regularly shaped agglomerate nanoroads with average diameter approximately 300 nm. After chemical etching reaction, the SEM of obtained BiOI/CdWO$_4$ heterjunction with tight and jagged structure is shown in Figure 2c. The BiOI particles are randomly covered on the surface of CdWO$_4$ nanoroads, indicating the integration of BiOI and CdWO$_4$. In addition, the elements of O, Bi, I, W, and Cd are detected in the BiOI/CdWO$_4$ composite sample by the EDS spectrum, confirming that CdWO$_4$ was successfully combined with BiOI, and the EDS analysis were show in Figure.2d.

To further detect the BiOI/CdWO$_4$ heterostructure structure, BC-2.0 was characterized by TEM and HRTEM. The Figure.2e confirms that the product is assembled by BiOI nanoparticles supported on the surface of the nanorods of CdWO$_4$. The Figure 2f shows the HRTEM image of the sample BC-2.0, there are two sets of lattice fringes shown in the spectra. The clear lattice fringe with an interval of 0.3012 nm can be indexed to (122) lattice plane of tetragonal BiOI and that of 0.1319 nm agreed with the (110) lattice plane of CdWO$_4$, which further demonstrated that the BiOI/CdWO$_4$ heterostructure structure were successfully synthesized. The results were consistent with what we have been obtained from the XRD results in Figure.1.

X-ray photoemission spectroscopy (XPS) all usually applied to investigate the surface composition and chemical state of the samples. From the Figure 3a, the Bi, O, I, Cd and W elements are clearly observed in the survey spectra. The peaks (Fig.3b) with two binding energy of 159.2 and 164.5 eV in the high resolution XPS spectrum of Bi 4f are attribute to Bi 4f7/2 and Bi 4f5/2, demonstrating that the main chemical state of Bi in the sample is +3 [29]. From Figure 3c, two peaks of I at 619.0 and 630.5 eV relate to the I 3d5/2 and I 3d3/2, respectively, at the meantime verify I in the sample is -1 [30], in good agreement with further references. The W 4f XPS spectrum illustrated in Fig. 3d two peaks at 35.37 eV and 37.62 eV will be found, indicated the value of W element in the sample present +6 [31]. The XPS spectrum of the O was show in Figure.3e, O main from BiOI, $CdWO_4$ and H_2O absorption on the surface of the sample [32]. The high resolution C 1 s spectrum has been discover in Figure.3f. The XPS results further prove the coexistence of BiOI and $CdWO_4$ in the BC-2.0 sample, which is consistent with the EDS analysis.

The DRS is often used to detect the optical absorption and energy band feature of semiconductors. The Figure 4a shows BiOI with strong absorption in the visible light range, with an absorption edge approaching 570 nm. However, from the $CdWO_4$ DRS analysis, there is no absorption in the visible light, which has also been reported in other literature [33]. However, compared with $CdWO_4$, BiOI/$CdWO_4$ heterostructures exhibit obvious absorption in the visible light, and is similar to the DRS of BiOI, for the reason of large BiOI loading in the composition. These results imply that the BiOI/$CdWO_4$ heterostructures can response to the visible light. So a lower band gap is

beneficial for electronic transitions, which subsequently results in an enhanced photocatalytic activity

The band gap energy (Eg) of samples were calculated by the following formula based on the DRS results [34]:

$$\alpha h\nu = A(h\nu - E_g)^{n/2}$$

In the formula, α, h, ν, A and E_g represent absorption coefficient, Planck constant, light frequency, a constant and band gap energy, respectively. Among of them, the value of n is determined by the type of optical transition of the semiconductor (i. e, n = 1) for direct transition and n = 4 for indirect transition). Based on the reports in literature, the value of n both BiOI and $CdWO_4$ are all 4 [35-36]. The Eg of BiOI and $CdWO_4$ can be calculated bythe plot of $(ah\nu)^{1/2}$ versus $(h\nu)$, which were 1.9 and 3.3eV, respectively. And the corresponding results were show in Figure.5b.

Moreover, the valence band (VB) edge position and the conduction band (CB) edge position of BiOI and $CdWO_4$ were also estimated according the following empirical formulas [37]:

$$E_{VB} = X - Ee + 0.5Eg$$

$$E_{CB} = E_{VB} - Eg$$

In the empirical formulas, E_{VB} is the valence band (VB) of semiconductor, E_{CB} is the conduction band (CB) of semiconductor, Ee is the energy of free electrons (about 4.5 eV), and Eg is the band gap energy of the semiconductor and X is the electro-negativity of the semiconductor. According to previous literature, the X values of BiOI and $CdWO_4$ are calculated to be 5.94 and 6.28 eV, respectively [38, 39]. The E_{VB}

values of BiOI and CdWO$_4$ were calculated are 2.39 and 3.45 eV, separately, and their K homologous E$_{CB}$ were estimated to be 0.49 and 0.15 eV, respectively. These results confirmed that BiOI and CdWO$_4$ was a perfectly composite structure, which was beneficial for the separation of the electron-hole (e$^-$-h$^+$) pair.

3.2. Enhanced photocatalytic activity and stability

The photocatalytic activity of the samples BiOI, CdWO$_4$ and heterostructures were evaluated by degradation by TC and RhB under visible light irradiation. The Figure 5a shows photocatalytic efficiency of the BiOI, CdWO$_4$ and BiOI/CdWO$_4$ heterostructures samples by photodegrading RhB. We can know that after 90 min irradiation under visible light, for the reason of CdWO$_4$ not responding under visible light so the degradation of the sample pure CdWO$_4$ can be neglect. The pure BiOI exhibits a weak degrade efficiency of 49.8％ after 90 min of visible light illumination and all of the BiOI/CdWO$_4$ heterostructures exhibit superior photocatalytic activity as compared to the pure BiOI and CdWO$_4$. As a comparative the sample of BT-2.0 were evaluated by degradation by RhB under visible light irradiation, and the result were show in Fig.S2. Among of the samples, BC-2.0 film showed the highest photocatalytic activity. In addition, the intensity of the peak at 553 nm gradually decreases with the irradiation time increased and they gradually decrease after 90 min as shown in Figure 5b. The maximum peak at k= 553 nm does not shift, which indicates that no intermediate generation are formed during the reaction.

The Figure 5c shows the degradation of TC with different samples under visible light. The pure BiOI and CdWO$_4$ exhibit very low photocatalytic activity, while the

two semiconductors were coupled together to construct heterojunction, the photocatalytic efficiency exhibit significantly enhanced. To further verify the enhanced photocatalytic activity of BiOI/CdWO$_4$ heterostructures via photodegrading TC. According to the previous studies, the photocatalytic degradation kinetics of TC was investigated, which can be ascribed to a pseudo-first-order reaction with a Langmuir-Hinshelwood model. And the initial concentration (C_0) of TC solution is small in Figure.5d:

$$Ln(C/C_0) = kt$$

In the formula C is the concentration of the TC at time t, C_0 is the primary concentration of TC, the slope k is the apparent reaction rate constant, higher k value indicates faster degradation rate. It can be found that the sample of BC-2.0 reveal higher rate constants than that of pure BiOI and CdWO$_4$. The sample of BC-2.0 with the maximum rate was almost 5 times as high as that of pure BiOI and 20 times of CdWO$_4$, respectively.

The above investigated results indicate the fact that a synergistic effect exists in the BiOI/CdWO$_4$ heterostructure photocatalysts. It should be attributed to the effective interfacial charge transfer resulted from the fabrication of a heterojunction, which will be discussed in details in the following photocatalytic mechanism section. Therefore, these results demonstrated that our photocatalyst can be a good candidate for application in environmental purification.

As is well known, at the photocatalytic oxidation process (POC), a series of reactive oxygen species, such as h$^+$, • OH and • O$_2^-$, are supposed to be involved. In

order to investigate the main species involved in RhB photodegradation over the BiOI/CdWO$_4$ composite, 1, 4-benzoquinone (BQ), disodium ethylene diaminetetraacetate (EDTA-2Na) and tert-butyl alcohol (IPA) were adding in the composition when we test of the catalyst activity, acting as the scavengers for •O$_2^-$, h+ and • OH, are introduced into the POC, respectively [40-42]. As show in Figure.6a and 6b, the photocatalytic degradation of RhB is obviously inhibited after the addition of BQ or EDTA. On the contrary, it is only slightly suppressed when IPA addition in the POC. The reactive species results indicate that h$^+$ and •O$_2^-$ were play important role in the photocatalytic degradation reaction.

To be more precise verify the generation of radicals reaction, the ESR were using dimethyl pyridine N-oxide (DMPO) as trapping agent play a role group, and the result were show in Figure. 6c and 6d. Before the measurement, the samples (10 mg) and DMPO (30 µL) were dispersed in deionized water and methanol, respectively. The Figure 6c shows that the black line is irradiated under the faint natural light and the red line is under the instrumental light. Six characteristic peaks from the DMPO-·O$_2^-$ adducts are the evidence that the superoxide radicals (·O$_2^-$) are formed during the photocatalytic reaction. The·O$_2^-$ signal intensity under the instrumental light is obviously stronger than that under the natural light, suggesting that the ·O$_2^-$ radicals are generated under a strong light. Besides, the DMPO-•OH all have been investigated, no ·OH signal intensity under the instrumental light irradiation before and after. Herein, we may safely draw the conclusion that, ·O$_2^-$ plays a major role in the reaction.

The Mott-Schottky equation was conducted to verify the flat band potential of the as-prepared $CdWO_4$ and BiOI. Base on the Mott-Schottky equation, a linear relationship of $1/C^2$ versus applied potential can be obtained, and the negative and positive slopes correspond to p and n type conductivities, respectively. With the previous reports, we know the $CdWO_4$ is an n-type semiconductor and BiOI is a p-type semiconductor [43-44]. Thus, the $BiOI/CdWO_4$ can be seen as an p-n heterogeneous structure, which would be very conductive to the photogenerated charges separation. As reported earlier, the flat band potential represents the apparent Fermi level of a semiconductor in equilibrium with a redox couple [45-47]. Therefore, we can propose the change of energy band structure of the two semiconductors before and after the contact as shown in Fig.7a and b. The Fermi level of $CdWO_4$ and BiOI are 0.17 and 1.74 V (vs AgCl), respectively. When $CdWO_4$ and BiOI were brought in contact, the Fermi level should be at equilibrium conditions, a p-n heterogeneous structure can be formed after the contacting of the n-type $CdWO_4$ and p-type BiOI. The excited electrons on CB of p-type BiOI effectively transfer to that of n-type $CdWO_4$ under the effect of internal electric field and then react with O_2 adsorbed on the surface of catalysts to produce reactive species $\cdot O_2^-$. However, the VB potential of BiOI is higher than that of $CdWO_4$, thus the photogenerated holes remain on the surface of BiOI and directly oxidize organic pollution. In this case, the formation of p-n heterojunction ($BiOI/CdWO_4$) could effectively separate the photoexcited electron-hole pairs and remarkably reduce the recombination of photogenerated charge carries. As a result, the BiOI/ $CdWO_4$ heterostructures exhibit better

photocatalytic activity than those of single $CdWO_4$ and BiOI for the degradation of organic pollutions under visible light irradiation. The proof of the enhance separation of photogenerated electrons and holes we can be verify through the PL and photocurrent.

According to the above discussion, the probable reactions occurring in the photodegradation of RhB are following:

$$BiOI \rightarrow BiOI(e^- + h^+)$$

$$CdWO_4(e^-) + O_2 \rightarrow \bullet O_2^-$$

$$e^- + \bullet O_2^- + 2H^+ \rightarrow H_2O_2$$

$$H_2O_2 + Organics \rightarrow \ldots\ldots \rightarrow Degradation\ product$$

$$BiOI(e^- + h^+) \rightarrow BiOI(e^-) + BiOI(h^+)$$

$$BiOI(h^+) + Organics \rightarrow \ldots\ldots \rightarrow Degradation\ products$$
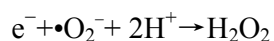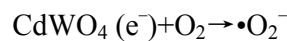
It is well known that the low PL intensity results a better charge separation of semiconductor materials [48]. The better photocatalytic activity of semiconductor is discussed and confirm by PL analysis. We can be know from Figure 9a, $CdWO_4$ and BC-2.0 exhibit an intense emission peak at about 470 nm. Compared with $CdWO_4$, the emission peak intensity of BC-2.0 decreases obviously, which suggests that the recombination of photogenerated charge carriers is inhibited extremely. Therefore, the PL verify that the efficient separation of the photoinduced charge carriers during the photocatalytic reactions. Fig.9b exhibits the PL spectra of the BC-2.0 and BT-2.0 under the excitation wavelength of 390 nm, and all the catalysts exhibit similar PL spectra which can be attributed to the band-band PL phenomenon with the energy of

light. Obviously, BT-2.0 shows the higher PL intensity than that of BC-2.0, indicating

that BC-2.0 compared with BT-2.0 the recombination of electron-hole pairs is

efficiently proved, which results in higher photodegradation efficiency. In order to

comparative PL quenching results of the $BiOI/CdWO_4$ and $BiOI/TiO_2$ heterojunctions

and their possible reasons. Base on the reference relative positions of the VB and CB

of $CdWO_4$, TiO_2, and BiOI all have been investigated, and the result were shown in

Fig. S2. From the Fig .S2a were we know for the purposes of $BiOI/TiO_2$ the

$\Delta_{CB(}BT\text{-}2.0_)=0.79$ Ev and $\Delta_{CB(}BC\text{-}2.0_) =0.34$ Ev. After the p-n junction were formed,

the $\Delta_{CB(}BT\text{-}2.0_)<\Delta_{CB(}BC\text{-}2.0_),$ so that the BC-2.0 recombination of electron-hole

pairs is efficiently proved for the PL quenching efficiently. At the same time, the

electric potential difference of VB all can explain the comparative degree of PL

quenching of the $BiOI/CdWO_4$ and $BiOI/TiO_2$ heterojunctions.

In order to further demonstrate that the high photocatalytic activity derived from

the the efficient separation of electrons-holes, the measured of photocurrents were all

have been investigated. From the Figure.9c, the photocurrent intensity of BC-2.0

exhibit highly compare with the sample of single BiOI. Base the photocurrent analysis

demonstrated that the high separation of photo-induced electrons and holes result

higher photocatalytic activity [49].

It has been widely known that the stability of semiconductor it is very important

for the practical application. The Figure 10a shows the catalyst exhibits slight loss of

activity after four recycles of the photo-degradation reaction. Due to the catalysts loss

lowly during the filtering and transferring processes, the amount of catalysts not

recovered. At the same time, p-n herjunction can efficiently decrease photo-corrosion of the catalysts. The results indicated that $BiOI/CdWO_4$ p-n heterostructure has a good photostability. In order to further testify the durability and stability of the catalysts, the catalysts were characterized by XRD analysis before and after photocatalytic, and the result shown in Fig. 10b. There was no obvious intensity chance after photocatalytic reaction, which all meant that the p-n herjunction of $BiOI/CdWO_4$ has good stability and recyclability for practical application.

Conclusions

A novel p-n herjunction were prepared by a simple chemical ultrasonic and stirring method and the composition exhibit efficiently enhance photocatalytic activity than the single BiOI and $CdWO_4$ for the degradation of TC and RhB under visible light irradiation. The reason of enhanced photocatalytic activity is attribution to the synergistic effects between BiOI and $CdWO_4$, and the efficient charge carrier transfer and separation of electron-hole. Moreover, photocatalytic mechanism investigations demonstrate that h^+ and $\cdot O_2^-$ play the key role in the $BiOI/CdWO_4$ p-n junction under visible light irradiation. The results demonstrated that in this work are expected for designing new p-n heterojunction photocatalyst and improving the performance of semiconductor photocatalysts for practical application.

References

1. K. M. Ji, J. G. Deng, H. G. Zang, J. H. Han, H. D. Arandiyan and H. X. Dai, Appl. Cata. B: Environmental, 2015, 165, 285-195.

2. S. Zhong, J. F. Zhang and W. Lu, RSC Advance, 2015, 5, 68646-68654.

3. Q. Sun, X. G. Jia and X. F. Wang, Dalton, T., 2015, 44, 14532-14539.

4. X. M. Jia, J. Cao, H. L. Lin, Y. Chen, W. F. Fu and S. F. Chen, J. Mol. Catal. A-Chem., 2015, 409, 94-101.

5. L. Liu, M. H. Huang, L. P. Long, Z. Sun, W. Zheng and D. H. Chen, Ceram. Int., 2014, 40, 11493-11501.

6. Y. Zhou, X. J. Zhang and Q. Zhang, J. Mater. Chem. A, 2014, 2, 16623-16631.

7. Y. J. Hao, F. T. Fa and F. Chen, Mate. Lett, 2014, 124, 1-3.

8. Y. Q. Wang, X. F. Cheng, X. T. Meng, H. W. Feng, S. G. Yang and C. Sun, J. Alloy., Compd., 2015, 632, 445-449.

9. R. P. Jia, G. X. Zhang, Q. S. Wu and Y. P. Ding, Appl. Surf. Sci., 2006, 253, 2038-2042.

10. A. M. Priya, R. K. Selvan, B. Senthilkumar, M. K. Satheeshkumar and C. Sanjeeviraja, Ceram. Int., 2011, 37, 2485-2488.

11. Aslam. Imran, C. B. Cao and Tanveer. M, RSC Advances, 2015, 5, 6019-6026.

12. W. N. Xu, C. H. Zeng, H. Hua, Q. Yang, L. Chen, Y. Xi and C. G. Hu, 2015, 327, 140-148.

13. X. F. Chang, S. B. Wang and Q. Qi, Appl., Catal, B-Environ, 2015, 176, 201-211.

14. L. Q. Ye, L. H. Tian, T. Y. Peng and L. Zan, J. Mater. Chem., 2011, 21, 12479-12484.

15. L. Q. Ye, L. Zan, L. H. Tian, T. Y. Peng and J. J. Zhang, Chem. Commun., 2011, 47, 6951-6953.

16. X. Xiao and W. D. Zhang, J. Mater. Chem., 2010, 20, 5866-5870

17. Y. Y. Li, J. S. Wang, H. C. Yao, L.Y. Dang and Z. J. Li, Catal Commun., 2011, 12, 660-664.

18. Y. Y. Li, J. S. Wang, B. Liu, L. Y. Dang, H. C. Yao and Z. J. Li, Chem. Phys. Lett, 2011, 508, 102-106.

19. L. Y. Wang, Daoud and Walid. A, Appl. Surf. Sci., 2015, 324, 532-537.

20. J. Jiang, X. Zhang, and P. P. Sun, J. Phys. Chem. C, 2011,115, 20555-20564.

21. T. Yan, M. Sun and H. Y. Liu, J. Alloy Compd., 2015, 634, 223-231.

22. K. H. Reddy, S. Martha and K. M. Parida, Inorg. Chem., 2013, 52, 6390-6401.

23. C. Liu and B. Chai, J. Mater. Sci-Mater. El., 2015, 26, 2296-230424.

24. C. G Li, Y. Zhao, F. F. Li, Z. Shi and S. H. Feng, Chem. mater, 2010, 22, 1901-1907.

25. C. G Li, T. Y. Bai, F. F. Li, L. Wang, X. F. Wu, L. Yuan, Z. Shi and S. H. Feng, CrystEngcomm, 2013, 15, 597-603.

26. T. Y. Bai, C. G. Li, F. F. Li, Zhao. L, Wang. Z. R, H. Haung, C. L. Chen, Y, Z. Han Shi and S. H. Feng, 2014, 6, 6782-6789.

27. C. G Li, Bai. T. Y, T. Li, F. F. Li, W. J. Dong, Z. Shi and S. H. Feng, Eur. J. Inorg. Chem., 2012, 2012, 1204-1209.

28. D. Ye, D. Z. Li and W. J. Zhang, J. Phys. Chem. C, 2008, 112, 17351-17356.

29. F. Dong, S. C. Lee, Z. B. Wu, Y. Huang, M. Fu, W. K. Ho, S. C. Zou and B. Wang, J. Hazard. Mater, 2011, 195, 346-354.

30. J. Cao, X. Li, H. L. Lin, S. F. Chen and X. L. Fu, J. Hazard Mater., 2012, 316, 239-240.

31. Y. Peng, Q. Guo. Chen, D. Wang, H. Y. Zhou and A. W. Xu, CrystEngComm, 2015, 17, 569-576.

32. Y. Wang, J. Ma, J. Tao, X. Zhu, J. Zhou, Z. Zhao and L. Xie, H. Tian, Ceram. Int., 2007, 33, 1125-1128.

33. Y. C. Ling, L. Zhou, L. Tan, Y. H. Wang and C. Z. Yu, CrystEngComm, 2010, 12, 3019-3026.

34. G. Liu, L. Wang, H. G. Yang, H. M. Cheng and G. Q. Lu, J. Mater. Chem., 2010, 20, 831-843.

35. J. Cao, B. Y. Xu, H. L. Liu and S. F. Chen, Chem Eng J., 2013, 228, 482-488.

36. L. R. Hou, L. Lian, L. H. Zhang, T. Wu and C. Z. Yuan, RSC Adv., 2014, 4, 2374-2381.

37. J. G. Yu, J. Zhang and M. Jaroniec, Green Chem., 2010, 12, 1611-1614.

38. D. Li, X. J. Bai and J. Xu, Phys. Chem. Chem Phys, 2014, 16, 212-218.

39. K. H. Reddy, S. Martha and K. M. Parida, Inorg. Chem., 2013, 52, 6390-6401.

40. T. B. Li, G. Chen, C. Zhou, Z. Y. Shen, R. C. Jin and J. X. Sun, Dalton Trans., 2011, 40, 6751-6758.

41. Y. Chen, S. Yang, K. Wang and L. Lou, J. Photochem. Photobiol., A, 2005, 172, 47-54.

42. M. Yin, Z. Li, J. Kou and Z. Zou, Environ. Sci.Technol., 2009, 43, 8361-8366.

43. J. J. Xu, M. D. Chen and Z. M. Wang, Dalton Trans., 2014, 43, 3537-3544.

44. W. C. Xu, J. Z. Fang, X. M. Zhu, Z. Q. Fang and C. P. Cen, Mater Recs Bull., 2015, 327, 140-148.

45. Yeh. T. F, Chan. F. F, Hsieh. C. T, Teng. H, J. Phys. Chem. C, 2011, 45, 22587-22597.

46. Kamat. P. V, J. Phys. Chem. C, 2008, 48, 18737-18753.

47. S. M. Sun, W. Z. Wang, D. Z. Li, L. Zhang, D. Jiang, ACS Catal., 2014, 4, 3498-3503.

48. J. Jiang, X. Zhang, P. B. Sun and L. Z. Zhang, J. Phys. Chem. C, 2011,115, 20555-20563.

49. S. Q. Liu, H. Z. Liu, G. H. Jin and H. Yuan, RSC Advance, 2015, 5, 45646-45653.
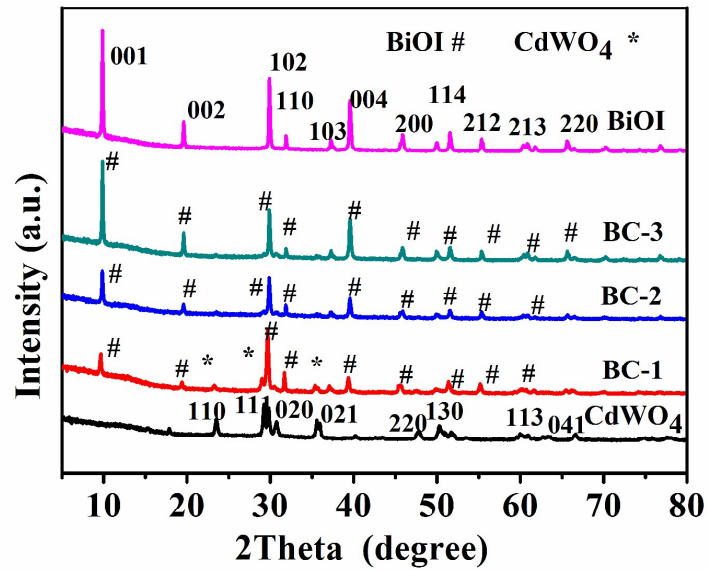
Figugre.1. XRD patterns of the samples: BiOI, $CdWO_4$ and different BiOI/$CdWO_4$

herojunction composition.
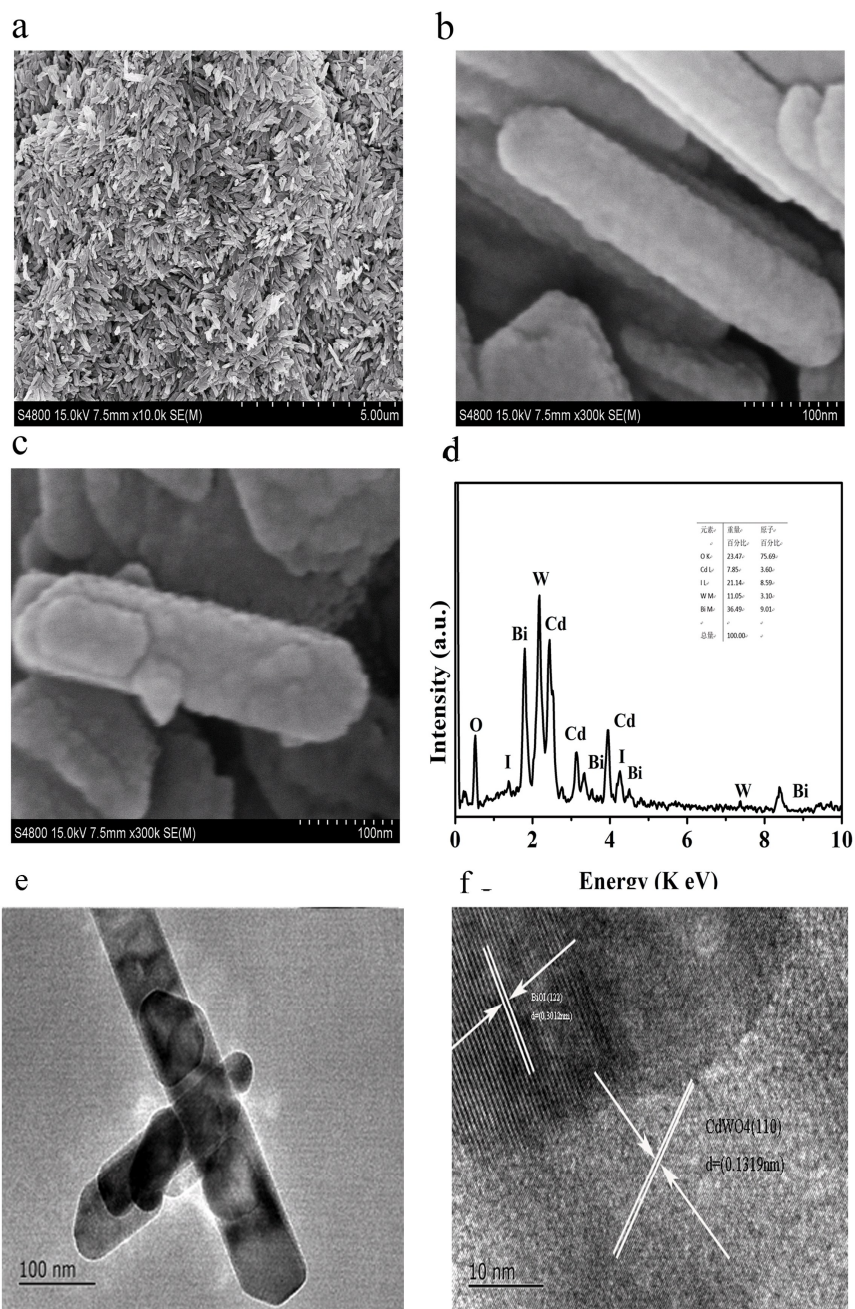
Figure.2. SEM images of the samples (a) $CdWO_4$, (b) the large version of $CdWO_4$, (c)

BC-2.0 and (d) EDS of the sample BC-2.0. TEM images of the sample BC-2.0. (e)

Low magnification TEM image; (f) high magnification TEM image
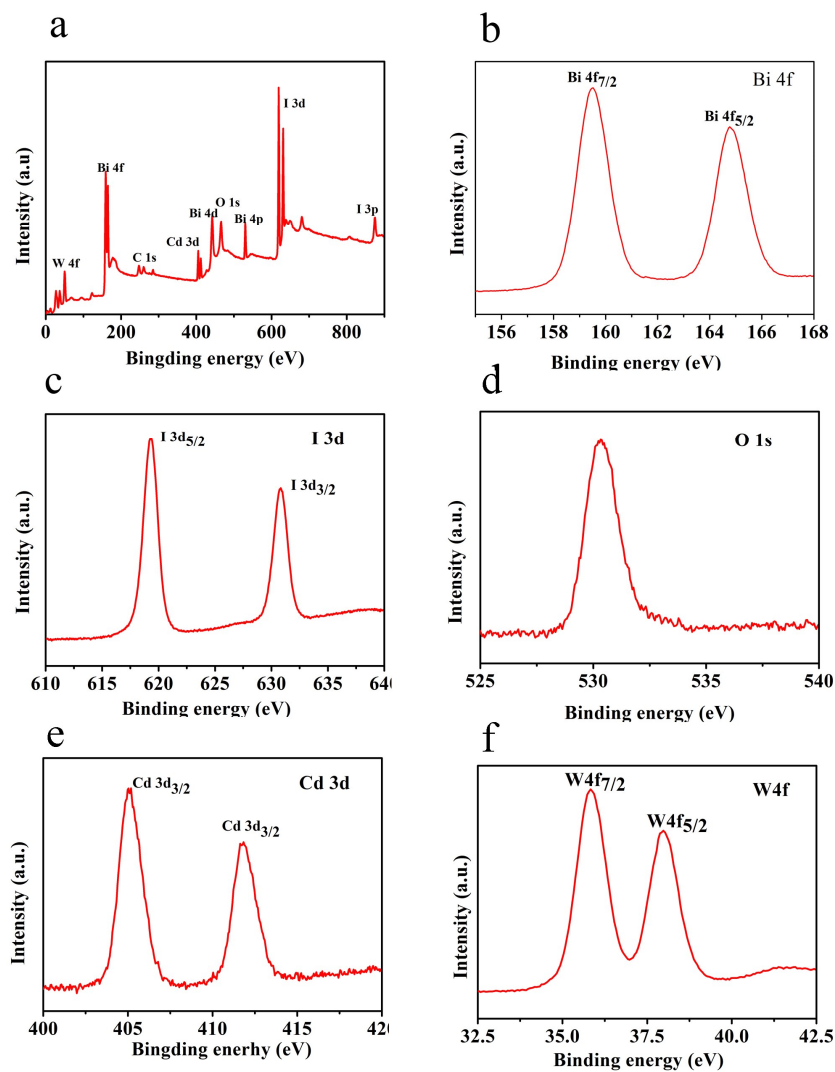
Fiure.3. XPS spectra of the BC-2.0 BiOI/CdWO$_4$ composite. (a) Survey of the sample; (b) Bi 4f; (c) I 3d; (d) O 1s; (e); Cd and (f) W 4f
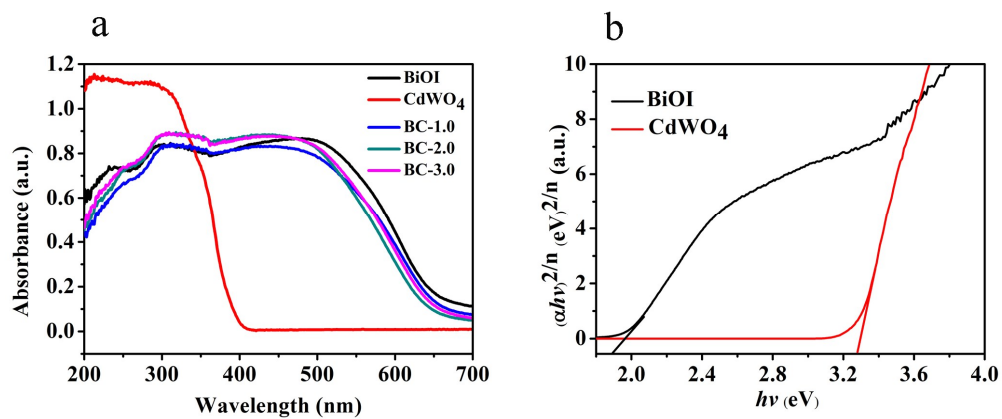
Fig.4. (a) UV-vis diffuse reflectance spectra of the as-prepared samples and (b) $(\alpha E_{photon})^{1/2}$ vs. E_{photon} curves of the as-prepared samples.
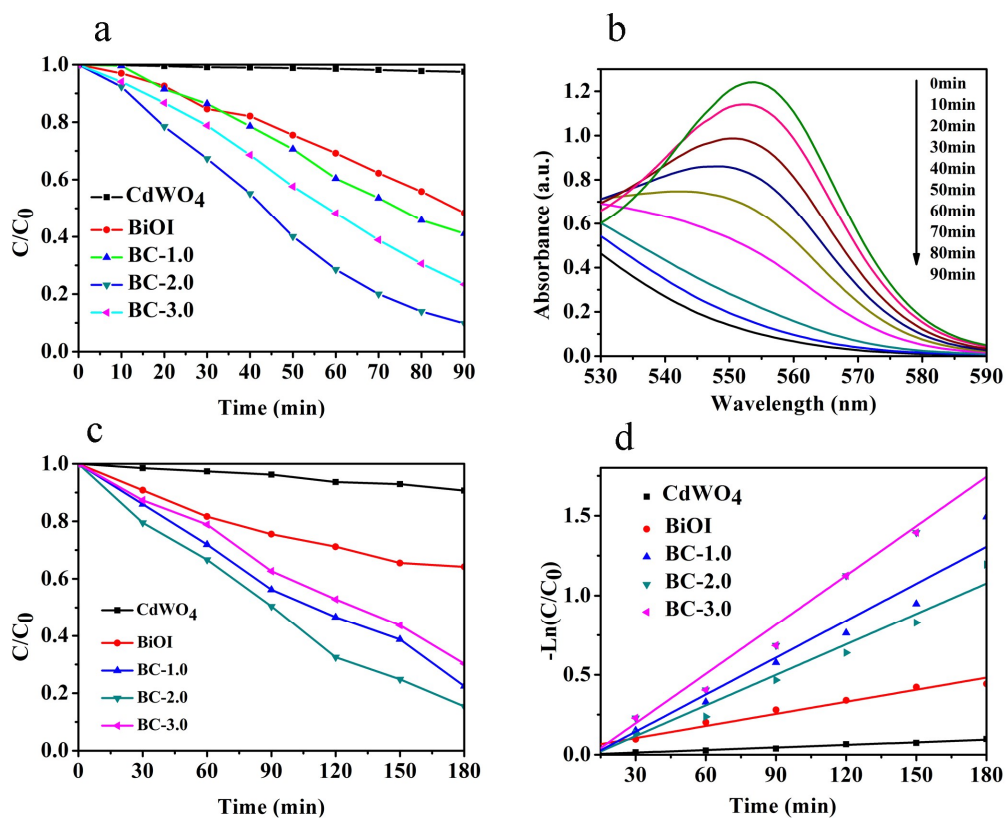
Figure.5. (a) comparison of photocatalytic activities of the samples for the degradation of RhB solution; (b) temporal UV-vis absorption spectral changes during the photocatalytic degradation of RhB in aqueous solution in the presence of the sample BC-2.0; (c) the TC degradation of the $CdWO_4$, BiOI, and $BiOI/CdWO_4$ (d) Pseudo-first-order kinetics curves of RhB degradation over different samples.
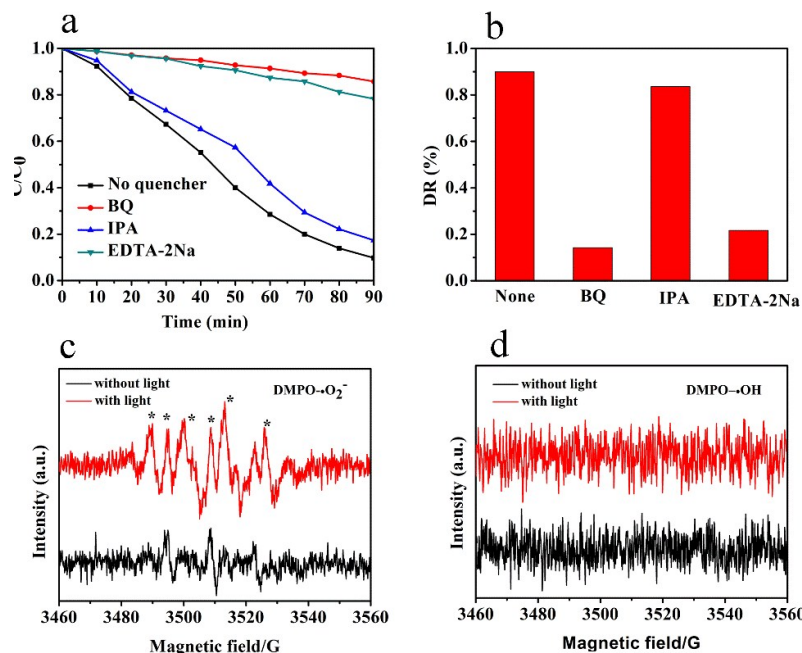
Figure.6. (a) and (b) The effect of reactive species on the photocatalytic degradation of RhB over BC-2.0 sample. DMPO spin-trapping ESR spectra in aqueous dispersion of BC-2.0 for (c) DMPO-•O_2^- (d) DMPO-•OH and irradiated for 90 s.
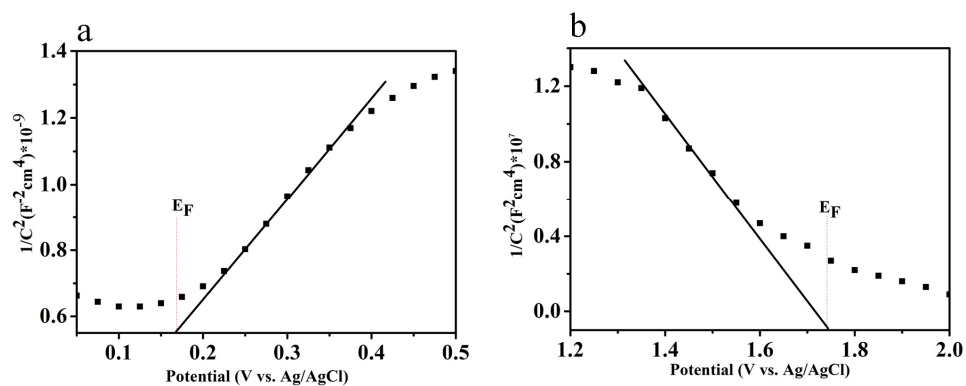
Fig.7.Variation of capacitance (C) with the applied potential in 0.5M Na_2SO_4 presented in the Mott-Schottky relationship for (a) mesoporous $CdWO_4$ and (b) pure BiOI. The capacitance was determined by electrochemical impedance spectroscopy
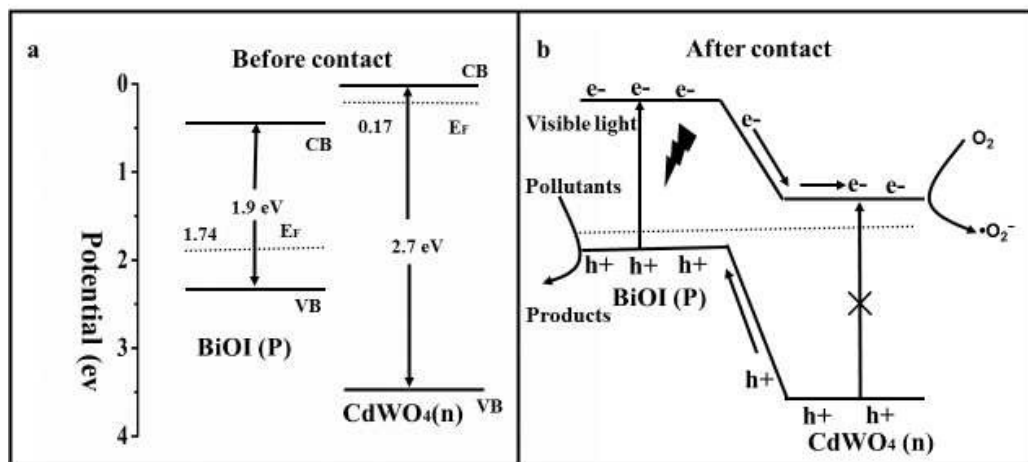
Figure.8. Schematic diagrams of energy band of $CdWO_4$ and BiOI before contact and

the formation of p-n junction and the proposed charge separation process.
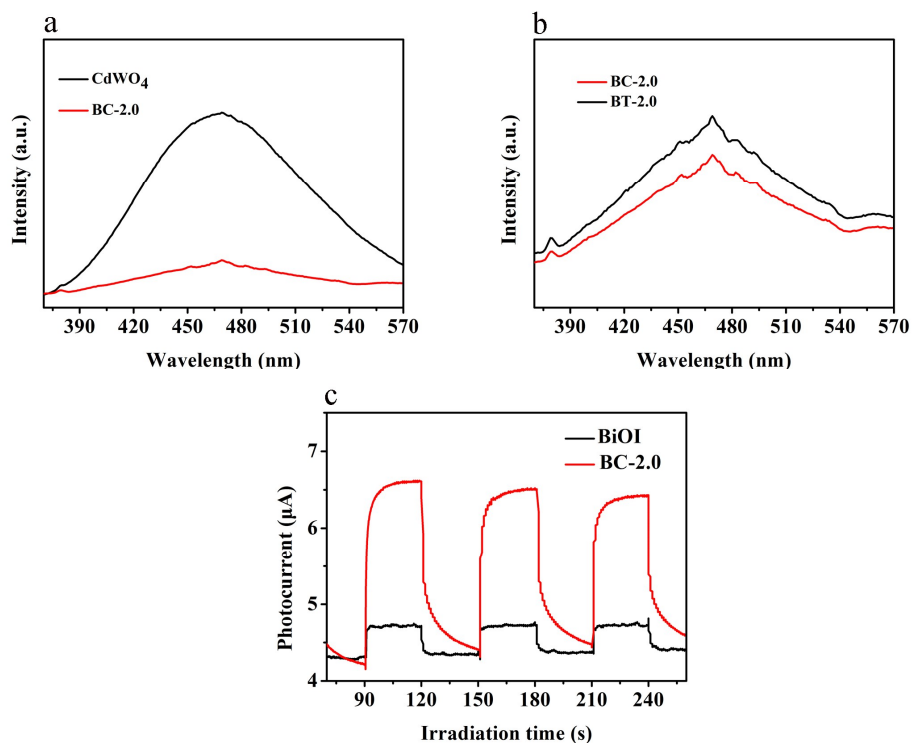
Figure.9. (a) PL emission spectra of CdWO$_4$ and BC-2.0 samples. (b) PL emission spectra of BC-2.0 and BT-2.0 samples (c) Transient photocurrent response for the pure BiOI and BC-2.0 composite.
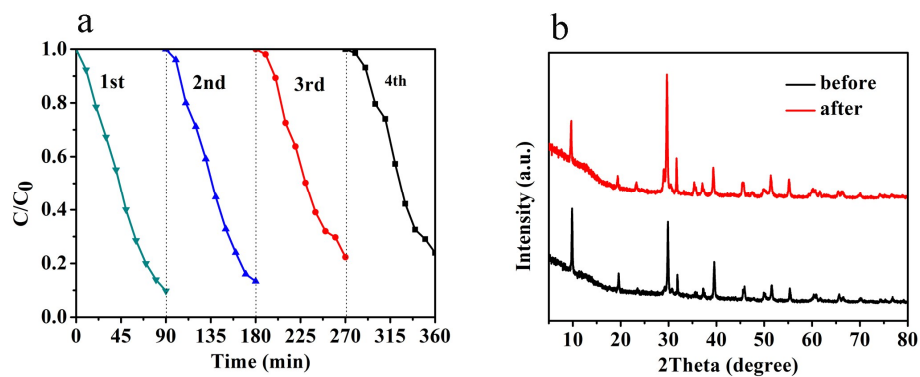
Figure.10. (a). Repeated photocatalytic degradation of RhB over BC-2.0 under visible

light irradiation. (b)XRD patterns of BC-2.0 before and after 6 h irradiation.

Graphical abstract